Full-Bridge LLC Resonant Converter with Series-Parallel Connected Transformers for Electric Vehicle On-Board Charger

Shen, Yanxia; Zhao, Wenhui; Chen, Zhe; Cai, Chengchao

Published in:
IEEE Access

DOI (link to publication from Publisher):
10.1109/ACCESS.2018.2811760

Publication date:
2018

Document Version
Publisher's PDF, also known as Version of record

IEEE Access
Multidisciplinary | Rapid Review | Open Access Journal

Received January 27, 2018, accepted February 26, 2018, date of publication March 5, 2018, date of current version March 28, 2018.

Digital Object Identifier 10.1109/ACCESS.2018.2811760

Full-Bridge LLC Resonant Converter With Series-Parallel Connected Transformers for Electric Vehicle On-Board Charger

YANXIA SHEN[1], (Member, IEEE), WENHUI ZHAO[1], ZHE CHEN[2], (Senior Member, IEEE), AND CHENGCHAO CAI[1]

[1]Engineering Research Center of IoT Technology and Application, Ministry of Education, Jiangnan University, WuXi 214122, China
[2]Department of Energy Technology, Aalborg University, 9220 Aalborg, Denmark

Corresponding author: Yanxia Shen (shenyx@jiangnan.edu.cn)

This work was supported in part by the National Natural Science Foundation under Grant 61573167 and Grant 61572237, and in part by the Fundamental Research Funds for the Central Universities under GrantJUSRP51510.

ABSTRACT A full-bridge LLC resonant converter with series-parallel connected transformers for an onboard battery charger of electric vehicles is proposed, which can realize zero voltage switching turn-on of power switches and zero current switching turn-off of rectifier diodes. In this converter, two same small transformers are employed instead of the single transformer in the traditional LLC resonant converter. The primary windings of these two transformers are series-connected to obtain equal primary current, while the secondary windings are parallel-connected to be provided with the same secondary voltage, so the power can be automatically balanced. Series-connection can reduce the turns of primary windings. Parallel-connection can reduce the current stress of the secondary windings and the conduction loss of rectifier diodes. Compared with the traditional LLC resonant converter with single transformer under same power level, the smaller low-profile cores can be used to reduce the transformers loss and improve heat dissipation. In this paper, the operating principle, steady state analysis, and design of the proposed converter are described, simulation and experimental prototype of the proposed LLC converter is established to verify the effectiveness of the proposed converter.

INDEX TERMS Series-parallel connected, full-bridge LLC resonant converter, dc-dc power conversion, on-board charger.

I. INTRODUCTION

Recently, there is a growing interest in electric vehicles (EV) because of the support of national policies and the threat of fossil fuel depletion, and the demand for on-board chargers is increasing rapidly [1], [2]. Small size, high efficiency and high reliability are common standards for evaluating the high-performance charger. In general, an EV battery charger is composed of two conversion stages as shown in Fig. 1, the first one is an AC/DC converter with PFC and the second one is an isolated DC/DC converter with wide voltage output for EV battery [3]–[8], the most common isolated DC/DC converters are the phase-shifted full-bridge (PSFB) converter and LLC resonant converter. High frequency soft-switching technology is often applied to the PSFB converter and LLC resonant converter for high efficiency and high power density. The output voltage of the PSFB converter can be regulated by using phase-shift control in a wide voltage range, but it is hard to realize ZVS for the lagging leg switches in light loads condition and there are the problem of duty cycle losses of secondary side [9], [10]. In contrast with PSFB converter, ZVS turn-on of all power switches and ZCS turn-off of all rectifier diodes can be realized in LLC resonant converter with higher efficiency [11]–[15], which makes LLC resonant converter more appropriate for electric vehicle on-board charger.

With the increase in the power level of the converter, power density decreases as transformer volume increases, the problem of heat dissipation also becomes increasingly serious, so some researchers proposed the topologies with two transformers substituting for single transformer. A flyback converter employing two transformers was proposed to implement a low-profile design [16]. The merits of the conventional single-transformer circuit are maintained, besides the transformer copper loss and the diode conduction

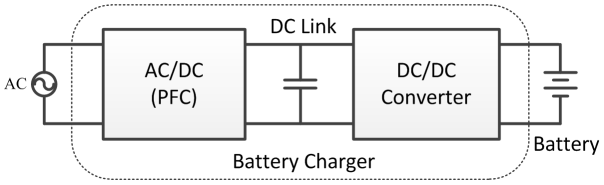

FIGURE 1. Typical circuit architecture of a battery charger.

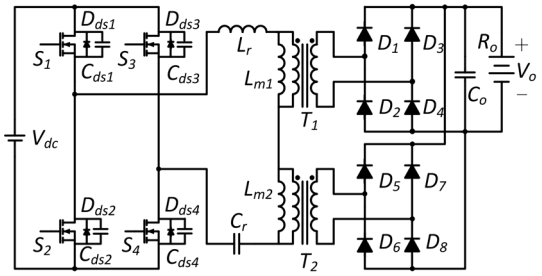

FIGURE 2. The proposed full-bridge LLC resonant converter.

loss are decreased by utilizing two separate transformers. These converters with two transformers series-parallel connected were presented in [17] and [18], the current stresses on transformer windings and copper losses are reduced by connecting the primary windings in parallel, while the secondary windings of two transformers are series-connected to reduce the winding turns and divide the output power equally. A half-bridge LLC resonant converter with two transformers parallel-series connected was proposed in [19], it is beneficial to improve the power density with using two small transformers instead of single large transformer. But the half-bridge structure is not suitable for high input voltage and high power applications. Similar to the converter in [19], a full-bridge LLC resonant converter with parallel-series connected transformers is proposed in [20], this structure is also beneficial to increase the power density and suitable for high input voltage and high power applications, but these converters with two transformers parallel-series connected have the imbalance problem of voltage caused by the transformer parameters inconsistency. A LLC resonant converter with double transformer series-parallel connection structure was proposed in [21] and [22], two transformers are used to reduce the power rating and the volume of each transformer core, and then the core loss can be decreased. Furthermore, heat generated from the core losses can also be shared evenly between two transformers, which is helpful to improve the heat dissipation and reliability. But the center-tapped winding structure is complex which leads to low utilization of the transformer cores. In addition, the voltage stress on the switches and the rectifier diodes is too high to be suitable for high-output-voltage and high-power applications.

In order to meet the application characteristics of electric vehicles charger with wide range of output voltage, high power rating, high efficiency and high reliability, a full-bridge LLC resonant converter with two small size transformers is proposed. On the primary side, the transformers are connected in series to obtain same primary current, while on the secondary side, they are connected in parallel to be provided with equal secondary voltage, so the power can be automatically balanced between two transformers. Two parallel full-bridge rectifier modules are utilized on the secondary side accordingly.

With this structure, we can get some advantages. Firstly, the copper loss can be decreased by reducing the turns of primary windings. Then, the conduction loss of rectifier diodes can be reduced because of the parallel-connection of the transformers on the secondary side which can reduce the current stress of rectifier diodes. Finally, the total power is shared equally between two transformers, and the height and volume of each core are reduced, so the heat dissipation and reliability are improved, which is of great practical significance in engineering applications, especially for high-power applications. Besides, the proposed converter has the same advantages as the LLC resonant converter with single transformer. All these advantages make the proposed LLC converter suitable for on-board charger applications.

This paper is organized as follows. In Section II, the circuit configuration and operation principle analysis of the proposed LLC converter are given. In Section III, the steady-state analysis of the converter is discussed. In Section IV, the charging profile, parameter design and loss analysis of the LLC converter are illustrated. The simulation and experimental results are given to prove the effectiveness of the proposed converter in Section V. Finally, some conclusions are drawn in Section VI.

II. CIRCUIT CONFIGURATION AND OPERATION PRINCIPLE

The configuration of the proposed full-bridge LLC resonant converter is shown in Fig. 2, which consists of the switching network, the resonant tank, the output rectifier- filter circuit. The switching network consists of switches S_1-S_4, with their parasitic anti-paralleled diodes D_{ds1}-D_{ds4} and parasitic capacitances C_{ds1}-C_{ds4}. The resonant tank is composed of a resonant inductor L_r, two magnetizing inductors L_{m1} and L_{m2}, a resonant capacitor C_r.T_1 and T_2 are two same isolated transformers with turns ratio $n_1 = n_2$, L_r is the total primary leakage inductance of T_1 and T_2. The output-rectifier-filter circuit includes the rectifier diode D_1-D_8, output-filter capacitor C_o. The input voltage V_{dc} of the proposed LLC converter is the output voltage of the AC/DC stage of the battery charger, V_o devotes the output voltage of the proposed LLC converter.

To simplify the analysis, it is assumed that both of the transformers are with the same magnetizing inductances and turns ratio, that means $L_{m1} = L_{m2}$ and turns ratio $n_1 = n_2 = n$, four switches are identical that the parasitic capacitances $C_{ds1} = C_{ds2} = C_{ds3} = C_{ds4}$, C_o is large enough to get a constant output voltage V_o.

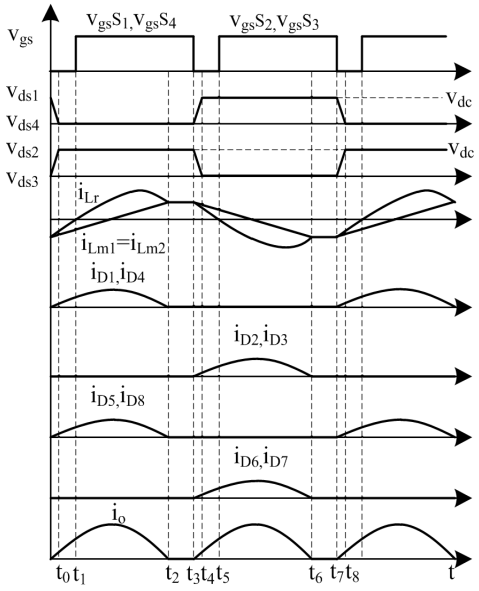

FIGURE 3. The key waveforms of the proposed converter.

The output voltage V_o varies with the switching frequency f_r of the LLC resonant converter. When the energy transfers from the primary side to the secondary side of transformers, the magnetizing inductors L_{m1} and L_{m2} are clamped, resonance occurs between L_r and C_r, with the resonance frequency f_r.

$$f_r = \frac{1}{2\pi\sqrt{L_r C_r}} \tag{1}$$

If there is no energy transferred to the secondary side, the load will be supplied by discharging the output capacitor C_o, and resonance will occur in L_r, C_r, L_{m1} and L_{m2}, the second resonant frequency is f_m

$$f_m = \frac{1}{2\pi\sqrt{(L_r + L_{m1}+L_{m2})C_r}} \tag{2}$$

Pulse Frequency Modulation (PFM) is employed to regulate the output voltage of the proposed LLC resonant converter. The switching network turns on and off with 50% duty cycle at switching frequency f_s. When $f_m < f_s < f_r$, the circuit has 8 operation states in one cycle, the key waveforms of the proposed converter are shown in Fig.3, the topological equivalent circuits are given in Fig.4.

Mode 1(t_0-t_1): Before t_0, S_1, S_2, S_3 and S_4 are turned off. At $t = t_0$, D_{ds1} and D_{ds4} conduct, the drain-source voltages of S_1, S_4 decrease from V_{dc} to zero, which provides the conditions for ZVS turn-on. In this mode, the energy is transmitted from the primary side of transformers to the secondary side, resonance occurs between L_r and C_r, D_1, D_4, D_5 and D_8 conduct, resonant current i_{Lr} decreases sinusoidally in negative direction, the voltages of L_{m1} and L_{m2} are clamped to nV_o, the magnetizing currents i_{Lm1} and i_{Lm2} decrease linearly in negative direction ($i_{Lm1} = i_{Lm2} = i_m$), the primary currents of transformers equal to $i_{Lr} - i_m > 0$.

Mode 2($t_1 - t_2$): At $t = t_1$, ZVS turn-on of switches S_1, S_2 are realized. In this mode, resonant current i_{Lr} changes sinusoidally in the positive direction. Since D_1, D_4, D_5 and D_8 conduct, the voltages of L_{m1}, L_{m2} are still clamped to nV_o, primary currents of transformers equal to $i_{Lr} - i_m > 0$, the energy is transmitted from input to the load, the resonant frequency is f_r.

Mode 3($t_2 - t_3$): At $t = t_2$, L_{m1} and L_{m2} begin to participate in resonance with C_r and L_r, the resonant frequency becomes f_m, the magnetizing currentsi_{Lm1} and i_{Lm2} rise and equal to the resonant current i_{Lr}, the primary currents of two transformers equal to zero. In this mode, the load is supplied by the output-filter capacitor C_o, the energy of primary side is no longer transmitted to secondary side. Since D_1, D_4, D_5 and D_8 turn off naturally with ZCS, the reverse recovery loss is eliminated.

Mode 4($t_3 - t_4$): At $t = t_3$, S_1 and S_4 are turned off. In this mode, the parasitic capacitors C_{ds1}, C_{ds4}, C_{ds2} and C_{ds3} resonate with L_r, C_{ds1} and C_{ds4} are charged through the resonant current i_{Lr} while C_{ds2} and C_{ds3} discharged. At $t = t_4$, the voltages of C_{ds1} and C_{ds4} rise to V_{dc}, while the voltages of C_{ds2} and C_{ds3} drop to zero.

Mode 5($t_4 - t_5$): At $t = t_4$, D_2, D_3, D_6 and D_7 are all in on-state, D_{ds2} and D_{ds3} conduct when parasitic capacitors complete the process of charging and discharging, the drain-source voltages of S_2 and S_3 are zero, which provides the conditions for ZVS. Resonance occurs betweenC_r and L_r, i_{Lr}, i_{Lm1} and i_{Lm2} decrease, the primary currents of transformers equal to $i_{Lr} - i_m < 0$, the voltages of magnetizing inductors L_{m1} and L_{m2} are -nV_o.

Mode 6($t_5 - t_6$): At $t = t_5$, ZVS turn-on of S_2 and S_3 are realized, $i_{Lr} = 0$. In this mode, resonance occurs between C_r and L_r with frequency f_r, The resonant current i_{Lr} varies in negative direction, i_{Lm1} and i_{Lm2} change linearly from positive to negative direction, the energy is transmitted from the primary side to the secondary side of two transformers.

Mode 7($t_6 - t_7$): At $t = t_6$, i_{Lm1} and i_{Lm2} equal to i_{Lr}, the resonant tank of C_r, L_r, L_{m1}, L_{m2} are resonant with frequency f_m, the energy of the primary side is not transmitted to the secondary side of two transformers , the load R_o is only supplied by C_o. The reverse recovery losses of diodes D_2, D_3, D_6 and D_7 are reduced because of ZCS turn-off.

Mode 8($t_7 - t_8$): At $t = t_7$, S_2 and S_3 are turned off, D_1, D_4, D_5 and D_8 are conducting. In this mode, resonance occurs among C_{ds1}, C_{ds4}, C_{ds2}, C_{ds3} and L_r, C_{ds2} and C_{ds3} are charged through resonant current i_{Lr} while C_{ds1} and C_{ds4} discharged. At t_8, the voltages of C_{ds2} and C_{ds3}rise to V_{dc}, the voltages of C_{ds1} and C_{ds4} drop to zero.

III. STEADY-STATE ANALYSIS OF THE PROPOSED LLC CONVERTER

The equivalent circuit of the proposed LLC converter is built by adopting first harmonic approximation (FHA) method [23] in Fig.5. Assuming that turns ratio of transformers T_1 and T_2 are defined as $n_1 = n_2 = n$, magnetizing inductors are defined as $L_{m1} = L_{m2} = L_m/2$, the

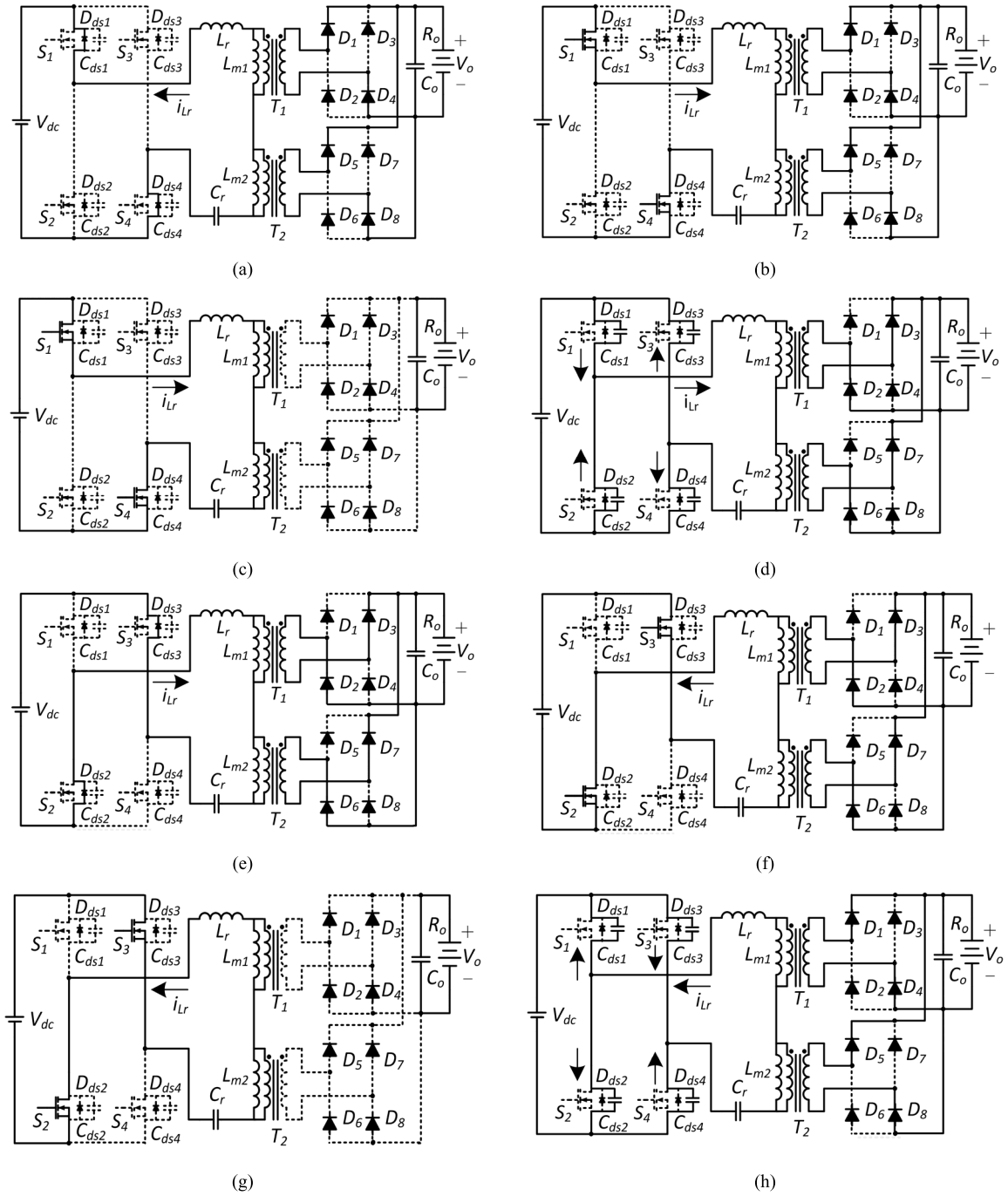

FIGURE 4. The Operation modes of the proposed converter. (a) Mode 1 ($t_0 - t_1$). (b) Mode2 ($t_1 - t_2$). (c) Mode 3 ($t_2 - t_3$). (d) Mode 4 (t_3-t_4). (e) Mode 5 ($t_4 - t_5$). (f) Mode 6 ($t_5 - t_6$). (g) Mode 7 ($t_6 - t_7$). (h) Mode 8 ($t_7 - t_8$).

ac equivalent resistance are defined as $R_{ac1} = R_{ac2} = R_{eq}/2$.$V_o$ and I_o denotes the output voltage and current respectively, the battery pack can be treated as a resistive load $R_o(R_o = V_o/I_o)$. The ac equivalent resistance of R_o can be derived as $R_{ac1} = R_{ac2} = 16n^2R_o/\pi^2$, the series equivalent resistance $R_{eq} = R_{ac1} + R_{ac2} = 32n^2R_o/\pi^2$.

A square-wave voltage as the input voltage v_{if} to the resonant tank is generated by the switching network. Based on Fourier analysis, $v_{if}(t)$ can be expressed as

$$v_{if}(t) = \frac{4V_{dc}}{\pi} \sum_{m=1,3,5...}^{\infty} \frac{1}{m} \sin(2\pi f_s m t) \tag{3}$$

The fundamental component of $v_{if}(t)$ is v_{if1}.

$$v_{if1} = (4V_{dc}/\pi) \sin(2\pi f_s t) \tag{4}$$

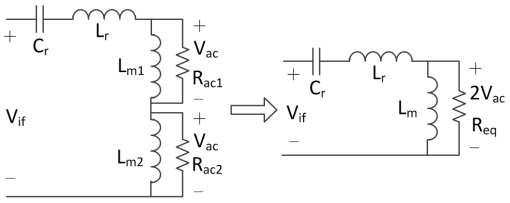

FIGURE 5. Equivalent circuit of the proposed converter.

The voltage of ac equivalent resistance is derived as $v_{ac} = (4nV_o/\pi)\sin(2\pi f_s t - \phi)$, where φ is the initial phase difference between resonant current and voltage.

According to the equivalent circuit shown in Fig. 5, the ac gain and input impedance of the circuit can be derived as equation (5) and (6) respectively.

$$M_{ac}(s) = \frac{2V_{ac}(s)}{V_{if1}(s)} = \frac{sL_mR_{eq}/(sL_m + R_{eq})}{1/(sC_r) + sL_r + sL_mR_{eq}/(sL_m + R_{eq})} \quad (5)$$

$$Z_{in}(s) = \frac{1}{sC_r} + sL_r + \frac{sL_mR_{eq}}{sL_m + R_{eq}} \quad (6)$$

Further, the dc voltage gain can be derived as

$$|M_{dc}M_{dc}(f_n, k, Q)| = \frac{1}{\sqrt{\left[1 + \frac{1}{k}\left(1 - \frac{1}{f_n^2}\right)\right]^2 + \left[Q\left(f_n - \frac{1}{f_n}\right)\right]^2}} \quad (7)$$

Where the quality factor Q is defined to be the ratio between the characteristic impedance Z_r and the series equivalent resistance R_{eq}, that is $Q = Z_r/R_{eq} = \sqrt{L_r/C_r}/R_{eq}$. The inductance coefficient is the ratio between magnetizing inductance and resonant inductance, that is $k = L_m/L_r$. The normalized frequency f_n is the ratio between switching frequency and resonant frequency, that is $f_n = f_s/f_r$.

When $R_{eq} \to \infty, Q = 0$, the no-load voltage gain is derived as

$$|M_{dc}(f_n, k)|_{open} = \frac{1}{1 + \frac{1}{k}\left(1 - \frac{1}{f_n^2}\right)} \quad (8)$$

From (8), when $f_n \to \infty$, the minimum gain can be obtained as $|M_{dc}(f_n, k)|_{open\_min} = k/(k+1)$.

The normalized input impedance of the resonant tank is as follows,

$$Z_n = \frac{Z_{in}}{Z_r} = \frac{1 - f_n^2}{jf_n} + \frac{jkf_n}{jkQf_n + 1} \quad (9)$$

By imposing the imaginary part of equation (9), the boundary condition between capacitive and inductive mode can be found as follows,

$$Q_z = \sqrt{\frac{1}{k(1 - f_n^2)} - \frac{1}{k^2 f_n^2}} \quad (10)$$

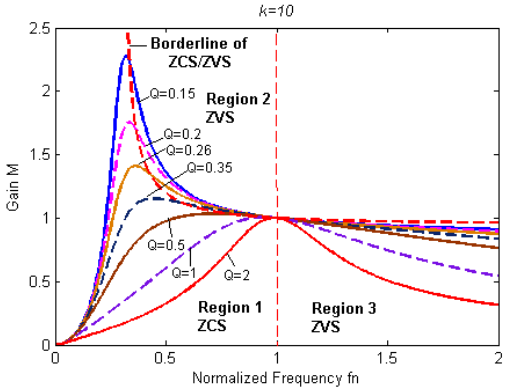

FIGURE 6. Characteristic curves of changing Q with fixed k.

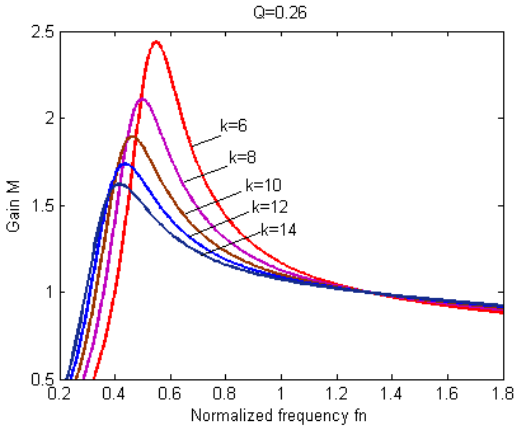

FIGURE 7. Characteristic curves of changing k with fixed Q.

$$M_z = \frac{f_n}{\sqrt{\left(1 + \frac{1}{k}\right)f_n^2 - \frac{1}{k}}} \quad (11)$$

From (7), it is known that the dc voltage gain is related to f_n, Q and k. To analyze the effect of Q and k on dc voltage gain, the effects of Q and k on the dc voltage gain can be discussed by using control variable method, the voltage gain curve is plotted by MATLAB. A family of plots of the voltage gain versus normalized frequency for different values of Q, with $k = 10$ is shown in Fig. 6. A family of plots of the voltage gain versus normalized frequency for different values of k, with $Q = 0.26$ is shown in Fig. 7.

Based on (11), the borderline of ZVS/ZCS can be plotted in Fig. 6. when $f_n < 1$, the equivalent impedance of the resonant tank is capacitive in region 1 but inductive in region 2. When $f_n > 1$, the equivalent impedance is inductive in region 3. This equivalent impedance condition determines the ZVS or ZCS operation of the converter, ZCS is realized in region 1,while ZVS is realized in region 2 and 3.

Changing Q under a fixed k as shown in Fig. 6, the voltage gain increases firstly and then decreases with the increase of the normalized frequency. Specially, when $f_n = 1$, the dc voltage gain maintains at 1 no matter how the load changes.

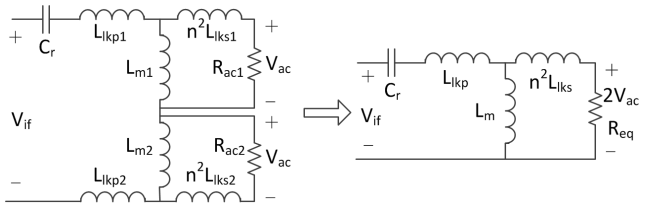

FIGURE 8. Equivalent circuit considering the secondary leakage inductance.

The larger Q is, the smaller peak of voltage gain is, and the narrower output voltage range is. However, the adjustable range of frequency of the LLC converter becomes narrower when Q is small.

As shown in Fig.7, changing k under a fixed Q, the change of voltage gain is the same as the analysis above. To increase the peak of voltage gain and expand the range of output voltage, k should be reduced as much as possible. However, if k is too small, the magnetizing current will increase when the input voltage is constant, which will make the loss of the resonant tank increase.

Therefore, both the gain curve and actual situation should be considered to decide k and Q. In general, LLC resonant converter is designed to operate in Region 2 and 3 because of ZVS operation.

Combined with the equivalent circuit model proposed in [24] and [25], the equivalent circuit of the proposed LLC converter with two transformers considering secondary leakage inductance is built in Fig. 8, L_{lkp1} and L_{lkp2} are the primary leakage inductance, L_{lks1} and L_{lks2} are the secondary leakage inductance. By assuming that

$$L_{lkp1} = L_{lkp2} = L_{lkp}, L_{lks1} = L_{lks2} = L_{lks}, k = L_m/L_{lkp},$$

then

$$L_p = L_{m1} + L_{lkp1} + L_{m2} + L_{lkp2} = 2(L_m + L_{lkp}) \tag{12}$$

$$\begin{aligned} L_r &= L_{lkp1} + L_{m1}//\left(n^2L_{lks1}\right) + L_{lkp2} + L_{m2}//\left(n^2L_{lks2}\right) \\ &= 2\left(L_{lkp} + L_m//\left(n^2L_{lks}\right)\right) \end{aligned} \tag{13}$$

According to the equivalent circuit in Fig. 8, the ac equivalent resistance can be obtained as follows,

$$\begin{aligned} Z'_{in}(s) &= \frac{1}{sC_r} + sL_r + \frac{sL_{m1}(n^2sL_{lks1} + R_{ac1})}{sL_{m1} + (n^2sL_{lks1} + R_{ac1})} \\ &\quad + \frac{sL_{m2}(n^2sL_{lks2} + R_{ac2})}{sL_{m2} + (n^2sL_{lks2} + R_{ac2})} \\ &= \frac{1}{sC_r} + sL_r + \frac{sL_m(sL_s + R_{eq})}{sL_m + (sL_s + R_{eq})} \end{aligned} \tag{14}$$

The gain can be simplified as

$$M = \frac{2V_{ac}}{V_{if1(s)}} = \left| \frac{f_sL_mR_{eq}C_r}{jf_s(1 - \frac{f_s^2}{f_r^2})(L_m + n^2L_{lks}) + R_{ac}(1 - \frac{f_s^2}{f_p^2})} \right| \tag{15}$$

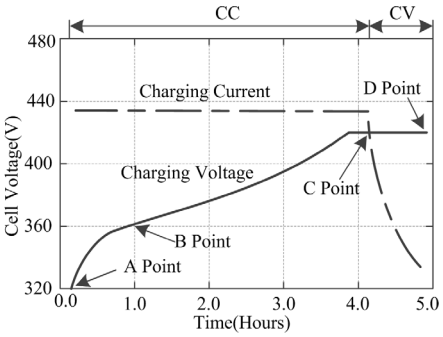

FIGURE 9. Charging profile of the Li-ion battery pack.

Where $L_p = L_m + L_{lkp}$, $L_r = L_{lkp} + L_m//\left(n^2L_{lks}\right)$,

$$f_r = \frac{1}{2\pi\sqrt{L_rC_r}}, \quad f_p = \frac{1}{2\pi\sqrt{L_pC_r}} \tag{16}$$

According to (15), the gain is fixed at resonant frequency, which is given as

$$M_{f_s=f_r} = \frac{L_m + n^2L_{lks}}{L_m} \tag{17}$$

As can be seen in (17), the gain at the resonant frequency is related to the magnetizing inductance, secondary leakage inductance and the turns ratio n. when n is too high, the gain will be greatly affected. For the transformer with high step-down turns ratio, the secondary leakage inductance cannot be ignored, otherwise it will bring large error between the theoretical gain and the actual one. In this proposed converter, the turns ratio n is less than 1, so the influence of the secondary leakage inductance is weak to be ignored.

IV. DESIGN OF THE PROPOSED CONVERTER

A. CHARGING PROFILE OF THE LI-ION BATTERY

The aim of the proposed LLC resonant converter is to charge a Li-ion battery pack from depletion voltage 320V to fully charging voltage 420V. The operating state of the converter varies with the voltage and current of the battery pack. Fig. 9 shows the charging profile of the Li-ion battery pack. There are four key operating points marked as A, B, C and D. The charging process with constant current(CC) 9.1A is from "A Point" to "C Point", and the charging process with constant voltage(CV) 420V is from "C Point" to "D Point". "A Point" indicates the start of charging, then the battery pack voltage rises rapidly to the nominal voltage 360V at "B Point", when the battery pack voltage reaches the maximum voltage 420V at "C Point", the charging process of CC turns into CV, and the CV charging process ends at "D Point" with the battery pack being fully charged.

B. PARAMETERS DESIGN OF THE PROPOSED LLC CONVERTER

In order to verify the theoretical analysis, the design specification of the proposed LLC converter is given in TABLE 1.

TABLE 1. Design specification for the rroposed LLC converter.

Parameter	Designator	Value
Input Voltage Range	V_{dc_min}~V_{dc_max}	380-420 V
Input Voltage Nominal	V_{dc_nom}	400 V
Output Power	P_o	3300 W
Switching Frequency Range	f_s	75-160 kHz
Primary resonant frequency f_r	f_r	110 kHz

V_{dc_nom} and V_{o_nom} denotes the rated input voltage and the rated output voltage respectively, turns ratio of transformers are defined as $n_1 = n_2 = n$, n can be calculated according to the following equation (18).

$$n = \frac{V_{dc\_nom}}{2(V_{o\_nom} + 2V_f)} \tag{18}$$

where V_f is the voltage drop on rectifier diode.

The minimum dc voltage gain is determined by the maximum input voltage and the minimum output voltage.

$$|M|_{\min} = \frac{2nV_{o\_\min}}{V_{dc\_\max}} \tag{19}$$

The maximum dc voltage gain is determined by the input minimum voltage and the maximum output voltage.

$$|M|_{\max} = \frac{2nV_{o\_\max}}{V_{dc\_\min}} \tag{20}$$

k and Q can be selected by combining the voltage gain curve with calculation, k is selected to 10 in this design. If the 95% margin is selected, Q can be calculated as,

$$Q = \frac{0.95}{k\,|M|_{\max}} \sqrt{k + \frac{|M|^2_{\max}}{|M|^2_{\max} - 1}} \tag{21}$$

The ac equivalent resistance can be given as,

$$R_{eq} = \frac{32n^2}{\pi^2} \frac{V^2_{onom}}{P_o} \tag{22}$$

Then, C_r, L_r, L_{m1} and L_{m2} are given as,

$$C_r = \frac{1}{2\pi f_r R_{eq} Q} \tag{23}$$

$$L_r = \frac{QR_{eq}}{2\pi f_r} \tag{24}$$

$$L_{m1} = L_{m2} = \frac{1}{2}L_m = \frac{1}{2}kL_r \tag{25}$$

C. LOSS ANALYSIS OF THE PROPOSED LLC CONVERTER

The LLC converter can achieve ZVS turn-on for power switches and ZCS turn-off for rectifier diodes, so the power loss is mainly from conduction losses, driving losses and switching losses of four MOSFET, conduction losses of eight rectifier diodes, the copper losses and core losses of two transformers. The following table lists the calculations of the various parts of the loss [26], [27].

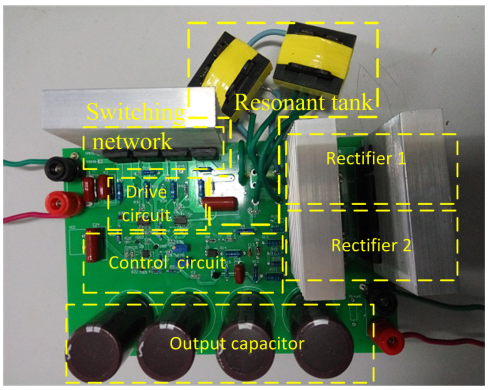

FIGURE 10. Laboratory prototype of the proposed converter.

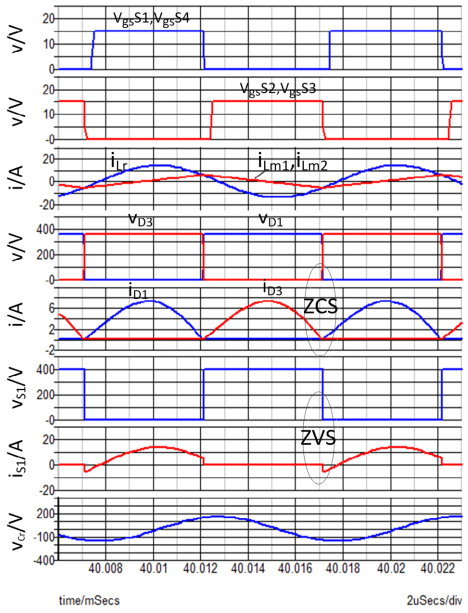

FIGURE 11. The simulation waveform at $f_s = f_r$ and rated $V_o = 360$V.

V. SIMULATION AND EXPERIMENTAL RESULTS

A prototype with output voltage range 320-420V and maximum output power 3300W is designed. The rated input voltage V_{dc} of the proposed converter from the AC/DC stage of on-board charger is 400V, the output voltage can be regulated from 320 to 420V, the output voltage at rated operating point is 360V, the resonance frequency f_r is 110kHz. In actual design, the resonant inductance L_r is the sum of leakage inductance of the two transformers, L_r is measured to be 14.6 uH, the magnetic cores of transformer are EE55. The picture of the prototype of the proposed converter is given in Fig. 10, the circuit component parameters are provided in Table. 3. Some theoretical simulation and experiment are carried out.

The simulation results of different working conditions are shown in Fig. 11-Fig. 14. $v_{gs}s_1$, $v_{gs}s_3$, $v_{gs}s_2$ and $v_{gs}s_4$ are the drive voltages of 4 switches, i_{Lr} is resonant current and i_{Lm1}, i_{Lm2} are magnetizing currents, v_{D1}, v_{D3} are voltages

TABLE 2. The losses calculations of the proposed LLC converter.

The component of LLC converter	The loss	Loss calculation
MOSFET	Driving loss	$P_{drive} = 4*(\frac{1}{2}C_{gs}V_{gs}^2)f_s$
	Turn-off loss	$P_{tf} = 4\frac{f_s v_i i_i (t_r + t_f)}{2}$
	Conduction loss	$P_c = P_{c\_mos} + P_{c\_body}$ $=4i_{mos\_rms}^2 R_{ds} + 4(V_d i_{anti\_ave} + i_{anti\_rms}^2 R_{body})$
Transformer	Core loss	$P_{core} = 2K_h f_s^m B_{ac}^n M_{core}$
	Copper loss	$P_{copper} = 2(i_{pri\_rms}^2 R_{ac\_pri} + i_{sec\_rms}^2 R_{ac\_sec})$
Rectifier diode	Conduction loss	$P_{c\_diode} = 8(\frac{1}{2}\frac{P_o}{V_o}V_F + i_{diode\_rms}^2 R_d)$

TABLE 3. Circuit component parameters.

Component	Symbol	Parameter
MOSFET	S_1~S_4	IPP60R125C6 (600 V/30 A)
Rectifier Diodes	D_1~D_8	STPSC2006CW (600 V/20 A)
Transformer Turns Ratio	n_1,n_2	0.55
Magnetizing Inductance	L_{m1},L_{m2}	73 *u*H (theoretical value 78 *u*H)
Resonant Capacitor	C_r	120 nF/*630* V (theoretical value 134 nF)
Output Capacitor	C_o	4*560 *u*F/*600* V
Resonant Controller		TI UCC25600

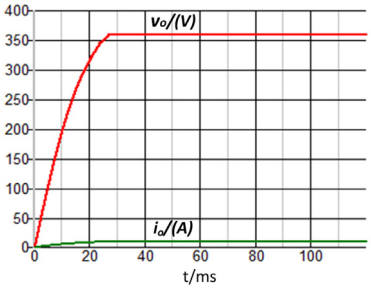

FIGURE 12. The simulation waveform of V_o and I_o at $f_s = f_r$.

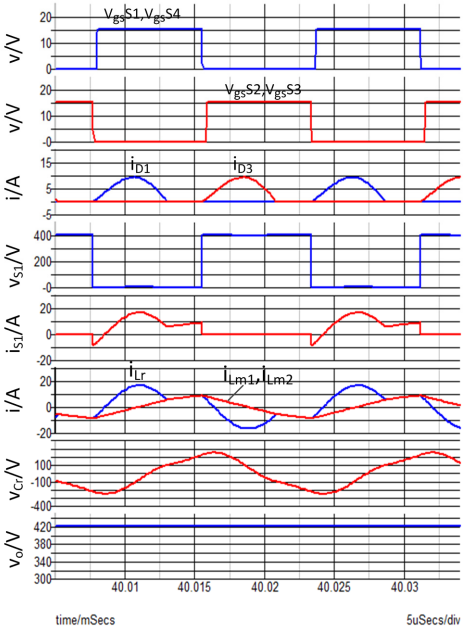

FIGURE 13. The simulation waveform at $f_s = 76$ kHz and $V_o = 420$V.

and i_{D1}, i_{D3} are currents of rectifier diodes D_1, D_3, v_{s1} is the drain-source voltage of S_1 and i_{s1} is the current through S_1, v_{Cr} is the voltage of resonant capacitor C_r.

From Fig. 11, it is easy to know that ZVS of power switches and ZCS of rectifier diodes have been realized at $V_o = 360$V. Fig. 12 shows the simulation results of output voltage and current when the switching frequency f_s equals to f_r, the voltage was stabilized at 360V and the current was 9.1A finally. The simulation results of the converter operating at the minimum output voltage and the maximum output voltage are shown in Fig. 13 and Fig. 14, ZVS of power switches were realized.

Some experimental waveforms at $V_o = 360$V, $f_s = f_r$ are shown in Fig. 15-Fig. 17. Fig. 15 shows the measured gate voltage waveform of MOSFETs S_1, S_2. As shown in Fig. 16, it can be observed that the drain-source voltage of MOSFET S_1 has been reduced to zero before the drive signal arrival, so switch S_1 was turned on at ZVS conduction. Fig.17 gives the measured voltage waveforms of rectifier diodes D_1-D_4, it shows that diodes achieved soft commutation without reverse recovery problem, so ZCS of these diodes has been realized. According to charging profile discussed in Section IV, voltage across resonant capacitor V_{Cr}, resonant current i_r and drain-source voltage of S_1 are shown in Fig. 18 when the converter operates at different operating points, it can be seen that the experimental results are the

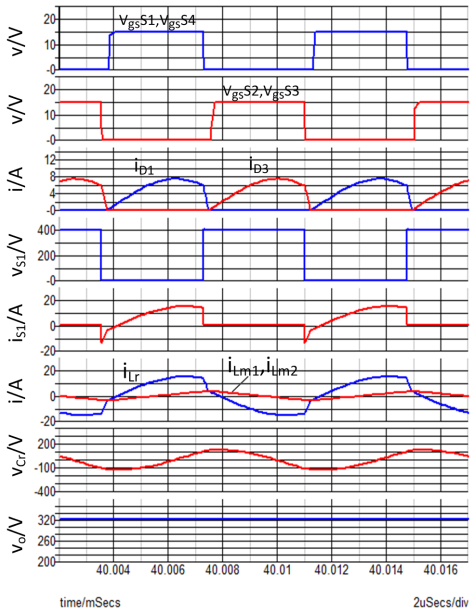

FIGURE 14. 14 The simulation waveform at $f_s = 155$ kHz and $V_o = 320$V.

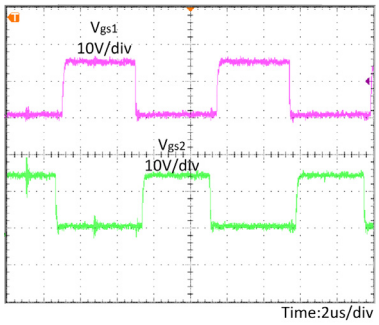

FIGURE 15. Gate voltage of MOSFET S_1, S_2 at $V_o = 360$V.

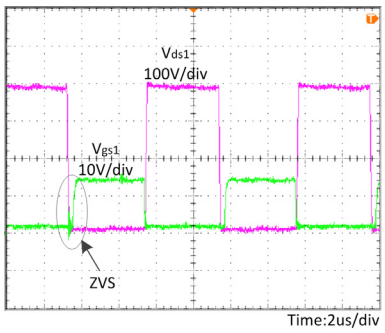

FIGURE 16. The gate voltage and drain-source voltage of MOSFET S_1 at $V_o = 360$V.

same as those of simulation. Fig. 19 gives the measured waveforms of the primary sides voltages of two transformers, it can be observed that two transformers connected in series at the primary side shared the input voltage equally.

The efficiency of the proposed LLC converter versus the LLC converter with single transformer at the same power

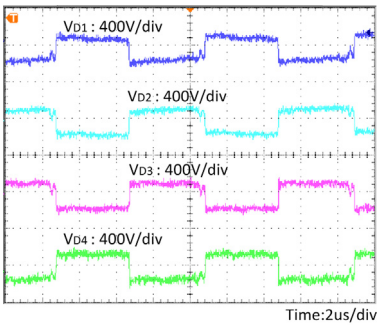

FIGURE 17. The measured voltage waveform of rectifier diodes $D_1 - D_4$ at $V_o = 360$V.

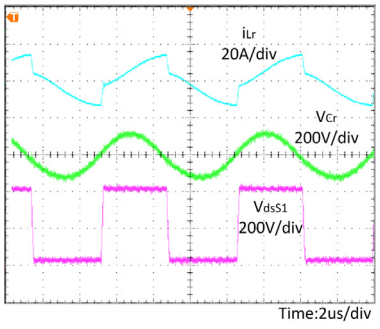

(a)

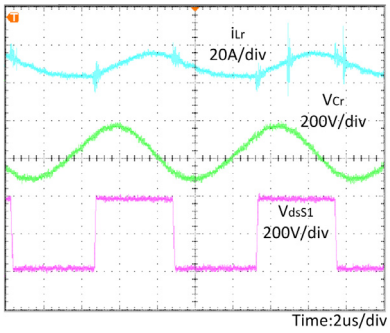

(b)

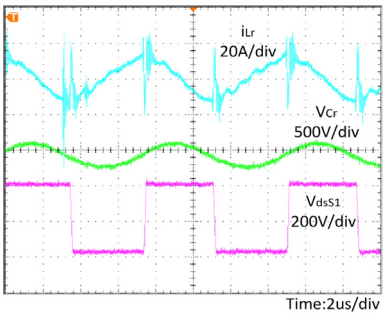

(c)

FIGURE 18. Experimental waveforms of the drain-source voltage of S_1, voltage of resonant capacitor C_r, resonant current i_{Lr} at $V_{dc} = 400$V.(a) $V_o = 320$V. (b) $V_o = 360$V. (c) $V_o = 420$V.

rating, input and output conditions is shown in Fig. 20. The proposed converter maintains good efficiency when the output voltage varies from 320V to 420V. The efficiency

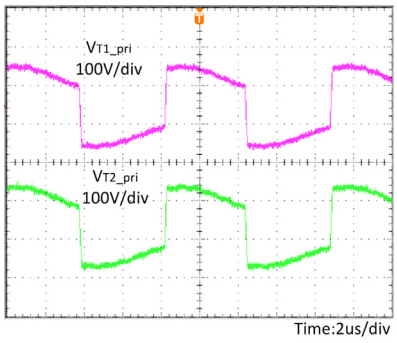

FIGURE 19. The primary sides voltages of two transformers at $V_{dc} = 400V$, $V_o = 360V$.

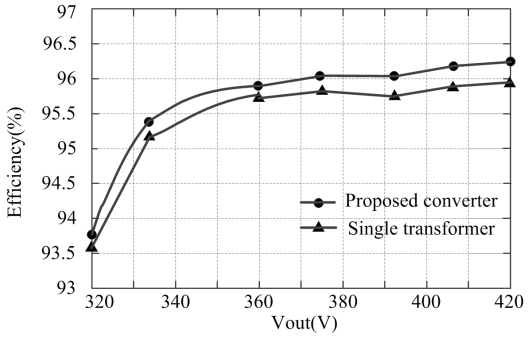

FIGURE 20. Efficiency of the proposed converter versus the converter of single transformer at $P_o = 3.3KW$, $V_{dc} = 400V$.

is always greater than the LLC converter with single transformer, the maximum efficiency of the proposed converter is about 96.31% at $V_o = 420V$. Besides, the volume of each core of two transformers is about 45% less than that of the single transformer at the same working condition and power rating, and the heat dissipation performance has been greatly improved. Therefore the LLC converter with two transformers is more beneficial in high-power onboard charger.

By comparing the above theoretical simulation results and experimental waveforms, it can be observed that ZVS-on of switches has realized when output voltage varies from 320V to 420V, and the steady-state input and output relations are basically consistent between theoretical and experimental results. It proved that the experiment results verify the effectiveness of the proposed converter based on the theoretical design.

VI. CONCLUSION

This paper presented a full-bridge LLC resonant converter with series-parallel connected transformers for electric vehicle on-board chargers. Two same transformers are series-connected at the primary side to obtain same primary current and parallel-connected at the secondary side to be provided with equal secondary voltage, so that the power can be automatically balanced between these two transformers. The structure of transformers series-parallel connected is more beneficial to reduce the size and losses of each core compared to conventional LLC converter with single transformer, which is of great help to improve the heat dissipation and efficiency. The working principle and steady-state analysis of the full-bridge LLC resonant converter with series-parallel connected transformers have been elaborated, then the design procedure and loss analysis were presented. The simulation and experimental results proved that the proposed LLC resonant converter has achieved ZVS-on for power switches, ZCS-off for rectifier diodes, wide output voltage range and high efficiency. Thus, the proposed converter can be employed in on-board charger applications. The future work will focus on the new topology of DC/DC converter with higher efficiency and higher power density for on-board charger.

REFERENCES

[1] S. Li, L. Tong, J. Xing, and Y. Zhou, "The market for electric vehicles: Indirect network effects and policy design," *J. Assoc. Environ. Resour. Econ.*, vol. 4, no. 1, pp. 89–133, Feb. 2017.

[2] R. Razi, B. Asaei, and M. R. Nikzad, "A new battery charger for plug-in hybrid electric vehicle application using back to back converter in a utility connected micro-grid," in *Proc. 8th Power Electron., Drive Syst. Technol. Conf.*, Apr. 2017, pp. 13–18.

[3] G. Kanimozhi, S. S. Kumar, and K. Likhitha, "Battery charger for automotive applications," in *Proc. Int. Conf. Intell. Syst. Control (ISCO)*, Nov. 2016, pp. 1–6.

[4] J. Deng, S. Li, S. Hu, C. C. Mi, and R. Ma, "Design methodology of LLC resonant converters for electric vehicle battery chargers," *IEEE Trans. Veh. Technol.*, vol. 63, no. 4, pp. 1581–1592, May 2014.

[5] R. Xu, W. Fang, X. D. Liu, Y. Liu, Y. Hu, and Y. F. Liu, "Design and experimental verification of on-board charger for electric vehicle," in *Proc. Int. Power Electron. Appl. Conf. Expo.*, Nov. 2014, pp. 1422–1427.

[6] W.-Y. Choi, M.-K. Yang, and H.-S. Cho, "High-frequency-link soft-switching PWM DC–DC converter for EV on-board battery chargers," *IEEE Trans. Power Electron.*, vol. 29, no. 8, pp. 4136–4145, Aug. 2014.

[7] D. S. Gautam, F. Musavi, M. Edington, W. Eberle, and W. G. Dunford, "An automotive onboard 3.3-kW battery charger for PHEV application," *IEEE Trans. Veh. Technol.*, vol. 61, no. 8, pp. 3466–3474, Oct. 2012.

[8] H. Wang, "A phase shift full bridge based reconfigurable PEV onboard charger with extended ZVS range and zero duty cycle loss," in *Proc. IEEE Appl. Power Electron. Conf. Expo. (APEC)*, Mar. 2016, pp. 480–486.

[9] B. Gu, J.-S. Lai, N. Kees, and C. Zheng, "Hybrid-switching full-bridge DC–DC converter with minimal voltage stress of bridge rectifier, reduced circulating losses, and filter requirement for electric vehicle battery chargers," *IEEE Trans. Power Electron.*, vol. 28, no. 3, pp. 1132–1144, Mar. 2013.

[10] D. S. Gautam, F. Musavi, W. Eberle, and W. G. Dunford, "A zero-voltage switching full-bridge DC–DC converter with capacitive output filter for plug-in hybrid electric vehicle battery charging," *IEEE Trans. Power Electron.*, vol. 28, no. 12, pp. 5728–5735, Dec. 2013.

[11] M. I. Shahzad, S. Iqbal, S. Taib, and S. Masri, "Design of a PEV battery charger with high power factor using half-bridge LLC-SRC operating at resonance frequency," in *Proc. IEEE Int. Conf. Control Syst., Comput. Eng. (ICCSCE)*, Nov. 2015, pp. 424–429.

[12] H. Y. Wang, S. Dusmez, and A. Khaligh, "Design considerations for a level-2 on-board PEV charger based on interleaved boost PFC and LLC resonant converters," in *Proc. IEEE Transp. Electrific. Conf. Expo (ITEC)*, Jun. 2013, pp. 1–8.

[13] Y. S. Dow, H. I. Son, and H.-D. Lee, "A study on half bridge LLC resonant converter for battery charger on board," in *Proc. 8th Int. Conf. Power Electron. ECCE Asia*, Jul. 2011, pp. 2694–2698.

[14] H.-G. Han, Y.-J. Choi, S.-Y. Choi, and R.-Y. Kim, "A high efficiency LLC resonant converter with wide ranged output voltage using adaptive turn ratio scheme for a li-ion battery charger," in *Proc. IEEE Vehicle Power Propuls. Conf. (VPPC)*, Oct. 2016, pp. 1–6.

[15] H. Xu, Z. Yin, Y. Zhao, and Y. Huang, "Accurate design of high-efficiency LLC resonant converter with wide output voltage," *IEEE Access*, vol. 5, pp. 26653–26665, Sep. 2017.

[16] Y.-K. Lo and J.-Y. Lin, "Active-clamping ZVS flyback converter employing two transformers," *IEEE Trans. Power Electron.*, vol. 22, no. 6, pp. 2416–2423, Nov. 2007.

[17] B.-R. Lin and H.-Y. Shih, "ZVS converter with parallel connection in primary side and series connection in secondary side," *IEEE Trans. Ind. Electron.*, vol. 58, no. 4, pp. 1251–1258, Apr. 2011.
[18] Y.-K. Lo, H.-J. Chiu, J.-Y. Lin, C.-F. Wang, C.-Y. Lin, and B. Gu, "Single-stage interleaved active-clamping forward converter employing two transformers," in *Proc. IEEE Appl. Power Electron. Conf. Exp. (APEC)*, Mar. 2013, pp. 1898–1905.
[19] B.-R. Lin and J.-Y. Dong, "ZVS resonant converter with parallel–series transformer connection," *IEEE Trans. Ind. Electron.*, vol. 58, no. 7, pp. 2972–2979, Jul. 2011.
[20] H. Zhou, L.-F. Ma, T.-F. Wang, and Z.-S. Wang, "Full-bridge LLC resonant converter with parallel-series connected transformers," *Power Electron.*, vol. 50, no. 4, pp. 54–56, Apr. 2016.
[21] Y.-H. Huang, T.-J. Liang, and W.-J. Wu, "Analysis and implementation of half-bridge resonant capacitance LLC converter," in *Proc. IEEE Int. Conf. Ind. Technol.*, Mar. 2016, pp. 1302–1307.
[22] J. J. Shi, J. M. Zhang, J. T. Long, and T. J. Liu, "A cascaded DC converter with primary series transformer LLC and output interleaved buck," *Trans. China Electrotech. Soc.*, vol. 30, no. 24, pp. 93–102, Dec. 2015.
[23] S. D. Simone, C. Adragna, C. Spini, and G. Gattavari, "Design-oriented steady-state analysis of LLC resonant converters based on FHA," in *Proc. Int. Symp. Power Electron., Elect. Drives, Autom. Motion*, May 2006, pp. 200–207.
[24] H. Choi, "Analysis and design of LLC resonant converter with integrated transformer," in *Proc. IEEE Appl. Power Electron. Conf.*, Feb. 2007, pp. 1630–1635.
[25] H. Li and Z. Y. Jiang, "On automatic resonant frequency tracking in LLC series resonant converter based on zero-current duration time of secondary diode," *IEEE Trans. Power Electron.*, vol. 31, no. 7, pp. 4956–4962, Jul. 2016.
[26] Z. Fang, T. Cai, S. Duan, and C. Chen, "Optimal design methodology for LLC resonant converter in battery charging applications based on time-weighted average efficiency," *IEEE Trans. Power Electron.*, vol. 30, no. 10, pp. 5469–5483, Oct. 2015.
[27] C.-H. Yang, T.-J. Liang, K.-H. Chen, J.-S. Li, and J.-S. Lee, "Loss analysis of half-bridge LLC resonant converter," in *Proc. Future Energy Electron. Conf.*, Dec. 2013, pp. 155–160.

YANXIA SHEN (M'02) was born in Zibo, China, in 1973. She received the M.S. degree in control theory and engineering from the Wuxi University of Light Industry, China, in 1999, and the Ph.D. degree in power electronics and motor drives from the China University of Mining and Technology, China, in 2004. From 2007 to 2008, she visited the Power Electronic Laboratory, University of California, Irvine, where she was with Professor K. M. Smedley. From 2015 to 2016, she visited the Department of Energy Technology, Aalborg University, Aalborg, Denmark, where she was involved with Professor Z. Chen.

She is currently a Full Professor with the School of IOT Engineering, Jiangnan University, Wuxi, China. She has authored or co-authored over 100 publications in her technical field. Her current research interests include motor drives, power electronics, charging technology of electric vehicle, and LED drives.

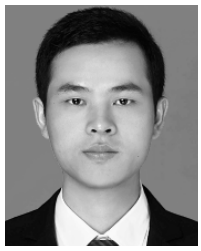

WENHUI ZHAO was born in Hubei, China, in 1991. He received the B.S. degree in electrical engineering from the Huazhong University of Science and Technology Wuchang Branch, in 2015. He is currently pursuing the M.S. degree in electrical engineering with Jiangnan University, Jiangsu, China.

His research interests include power electronics and charging technology of electric vehicle.

ZHE CHEN (M'95–SM'98) received the B.Eng. and M.Sc. degrees from the Northeast China Institute of Electric Power Engineering, Jilin, China, and the Ph.D. degree from the University of Durham, Durham, U.K.

He is currently a Full Professor with the Department of Energy Technology, Aalborg University, Aalborg, Denmark, where he is the Leader of the Wind Power System Research Program. He is also the Danish Principal Investigator for Wind Energy of the Sino-Danish Centre for Education and Research. He has authored or co-authored over 320 publications in his technical field. His current research interests include power systems, power electronics, electric machines, wind energy, and modern power systems.

Dr. Chen is a Fellow of the Institution of Engineering and Technology, U.K., and a Chartered Engineer in U.K. He is an Associate Editor (renewable energy) of the IEEE TRANSACTIONS ON POWER ELECTRONICS.

CHENGCHAO CAI was born in Jiangsu, China, in 1991. He received the B.S. degree in automation from Huaiyin Normal University, Huaian, China, in 2015. He is currently pursuing the M.S. degree in electrical engineering with Jiangnan University, Jiangsu. His research interests include power electronics and LED driver.